10. V. V. Bezrukikh, T. K. Breus, et al., "Dependence of magnetopause and bow shock positions on solar wind parameters and magnetopause plasma structure," Space Res., 16, 657 (1976).
11. Yu. D. Krisilov, V. V. Bezrukikh, et al., "A wide-angle charged particle energy spectrometer for investigating the solar wind on Prognoz 9," in: Scientific Apparatus for Space Research [in Russian], Nauka, Moscow (1986).
12. J. H. King (ed.), Interplanetary Medium Data Book, NASA-GSFC, Greenbelt, Maryland (1977).
13. K. I. Gringauz, V. V. Bezrukikh, et al., "Study of interplanetary ionized gas, energetic electrons, and corpuscular radiation from the sun using three-electrode charged-particle traps on the second Soviet space rocket," Dokl. Akad. Nauk SSSR, 131, No. 6, 1301 (1960).
14. G. A. Kotova, K. I. Gringauz, V. V. Bezrukikh, et al., "Solar wind speed as a function of distance from the heliospheric current sheet, based on data from Prognoz 9," Kosm. Issled. (1986).
15. J. T. Hoeksema, "Structure and evolution of large-scale solar and heliospheric magnetic fields," Doctoral Dissertation, CSSA-Astro-84-07, Stanford, California (1984).
16. Solar Geophysical Data, No. 488, Part 1 (1985).

SOLAR WIND SPEED AS A FUNCTION OF DISTANCE FROM THE HELIOSPHERIC CURRENT SHEET: DATA FROM PROGNOZ 9

G. A. Kotova, K. I. Gringauz, V. V. Bezrukikh,
M. I. Verigin, L. A. Shvachunova, V. Ridler,
and K. Shvingenshu

UDC 533.951.2

We compare the large-scale structure of recurrent high-speed streams in the solar wind with the large-scale structure of the heliospheric current sheet. The stream data were recorded by Prognoz 9 in 1983-1984. We perform a quantitative investigation of the solar wind speed V as a function of angular distance λ from the current sheet. Based on the entire data set of V measurements by Prognoz 9, the function $V(\lambda)$ can be approximated by the expression V (km/sec) = 410 + 305·$\sin^2\lambda$. We show that the scatter of the experimental points with respect to the approximate curve is reduced if we allow for the fact that the mean velocity of the solar wind on the path from the sun to the earth is smaller than the speed V which is measured at the earth's orbit.

Prognoz 9 made measurements of the solar wind during the time period from July 1983 to February 1984, on the decline phase of solar cycle No. 21. It is well known that during the decline phase of the preceding cycle (No. 20), large recurrent high-speed solar wind streams were observed in the ecliptic plane, lasting 5-6 solar rotations. In the preceding paper [1], we conoluded, from Prognoz-9 data, that regular high-speed structure has resumed in the solar wind in the decline phase of the current solar cycle. In the present article, we will compare the large-scale structure of these streams with the large-scale structure of the heliospheric current sheet, and we will investigate how the solar wind speed behaves as a function of angular distance from the current sheet.

The way in which solar parameters behave as a function of angular distance from the current sheet λ manifests itself as a function of heliolatitude at certain phases of the 11-yr solar cycle. This is being discussed actively at the present time (cf., e.g., [2-5]). The dependence of solar wind parameters on λ has not been established reliably. The reasons for this are entirely understandable: direct measurements of the solar wind are limited to the ecliptic plane, measurements of the wind speed by means of interplanetary scintilla-

Translated from Kosmicheskie Issledovaniya, Vol. 25, No. 1, pp. 93-102, January-February, 1987. Original article submitted November 10, 1985.

 0010-9525/87/2501-0080$12.50

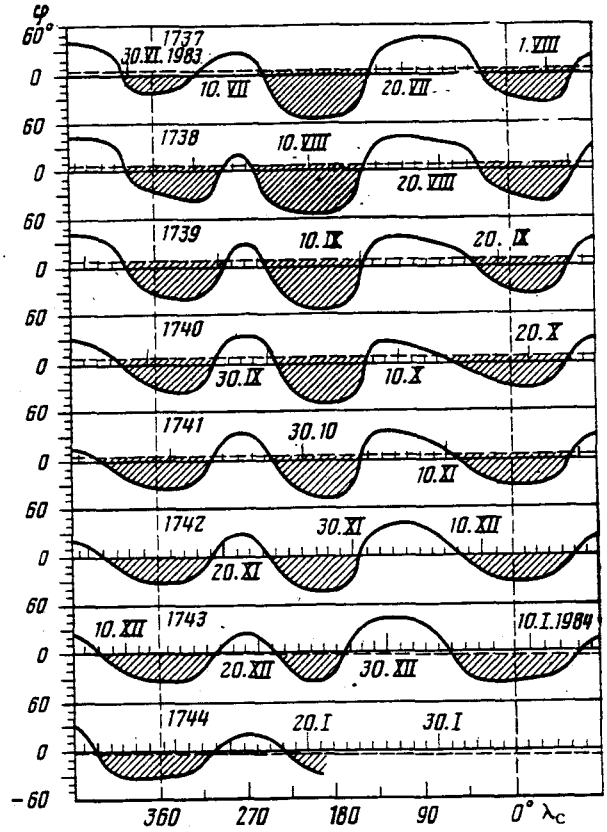

Fig. 1. Position of the heliospheric current sheet for 1983-1984. The coordinates are Carrington longitude λ_C and Carrington latitude φ_C. Along the abscissa axis, we also show the date in universal time. Vertical dashed lines denote boundaries of Carrington rotations No. 1737-1744.

tions yield only integrated results, and there are changes in the interplanetary medium which are generated by transients in the outer solar corona. (Among the latter are outward moving clouds of plasma, shock waves, eruptive prominences, etc.)

The fact that Prognoz 9 made measurements on the solar wind during the decline phase of solar activity (when the structure of the heliospheric current sheet is at its most regular, and the current sheet can be observed at significant distances from the ecliptic plane) makes it easier to determine how the solar wind parameters depend on the angular distance from the current sheet. (When solar activity is at a minimum, the heliospheric current sheet is limited to a narrow range of latitudes, and at maximum activity it is quite irregular [6]).

1. Analysis of Experimental Data. In the preceding article [1], it was mentioned that the high orbit of Prognoz 9 was unique in enabling us to obtain practically continuous information about large-scale formations in the solar wind. The satellite measured the ion component of the plasma by means of a D-137A modulation type of wide-angle energy spectrometer. Detailed descriptions of the features of the plasma experiment, and of the techniques used in reducing the data, can be found in [1, 7].

During the period of active operations of Prognoz 9, a regular structure of high-speed streams was observed in the solar wind (cf. Fig. 2 in [1]). This structure should obviously be related to the regular character of the large-scale magnetic field of the sun during the same time period, because the magnetic field controls the motion of plasma near the solar surface R_S, and the current lines are similar to the magnetic field lines. In order to analyze this relationship, it is convenient to make use of the ideas developed in [8, 9] concerning the concentric "source surface," R_{SS}.

In the approximate "source surface" model, it is assumed that in the spherical shell between R_S and R_{SS} the plasma has a negligible effect on the magnetic configuration (because

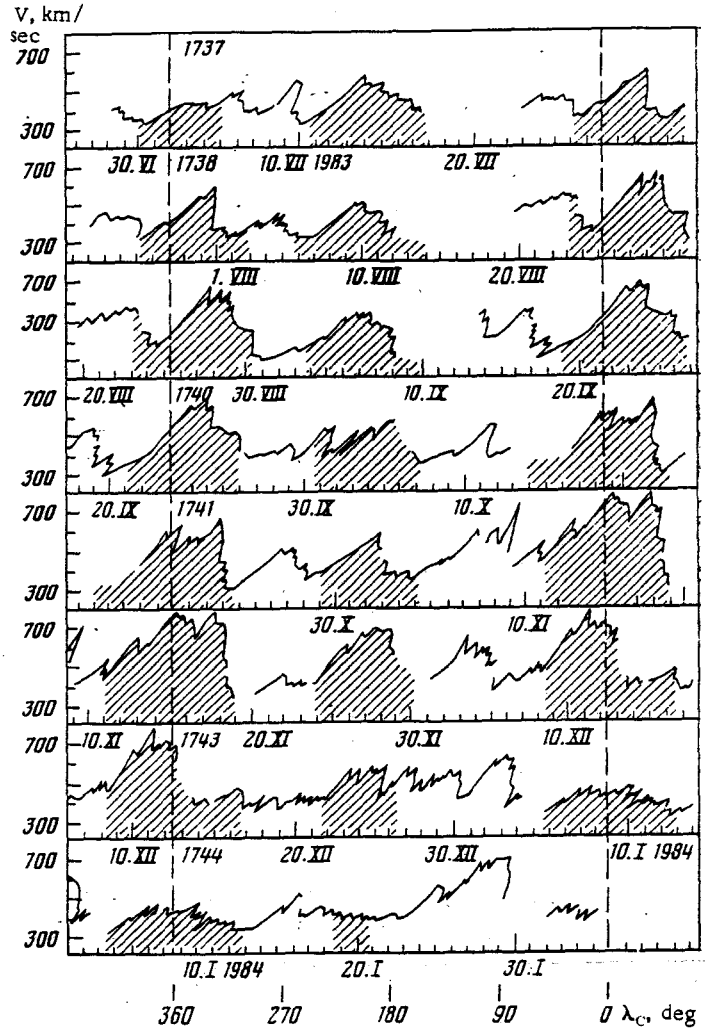

Fig. 2. Distribution of solar wind speed, obtained by projecting Prognoz 9 data along the satellite trajectory on the "source surface." Notation is the same as in Fig. 1.

the electric currents are small). Consequently, in the shell, the magnetic field B is obtained from a scalar magnetic potential which satisfies Laplace's equation. For radii $r > R_{ss}$, plasma effects predominate, and the lines of force take on a spiral form which is determined by the overall radial expansion of the plasma. Suitable boundary conditions must be chosen in order to solve the potential problem in the shell $R_s < r < R_{ss}$. For the boundary condition at $r = R_{ss}$, it is customary to choose the requirement that the magnetic potential be constant on that surface: this ensures that the magnetic field and the flow of plasma will be purely radial. For the boundary condition at $r = R_s$, we take the data of photospheric magnetic observations.

In Fig. 1 we present the results of calculating the position of the heliospheric current sheet for the time period which we are analyzing. These positions were calculated in [10] within the framework of a model where the "source surface" was located at $R_{ss} = 2.5R_s$. In these calculations, magnetic-field measurements along the line of sight were taken as the inner boundary conditions. The field data were obtained at the Stanford solar observatory. The dashed line in Fig. 1 shows the projection of the earth's orbit on the surface R_{ss}. Shaded areas denote time periods when this projection lies in the northern hemisphere of the sun relative to the interplanetary current sheet. During the decline phase of cycle No. 21, the large-scale magnetic field in the northern hemisphere of the sun was directed away from the sun.

In order to compare Prognoz-9 measurements of solar wind speed with the calculated position of the interplanetary current sheet [10], we must determine the heliographic longitude

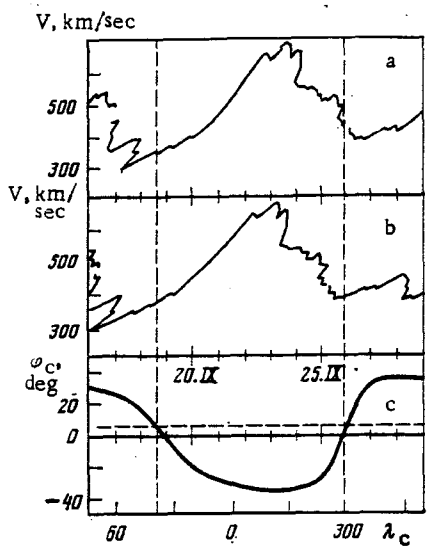

Fig. 5. Distribution of solar wind speed "projected" onto the "source surface." In (a) we assume <V> = V; in (b), we assume <V> = 0.85 V. c) Position of the current sheet. Here the horizontal dashed line indicates the projection of the satellite trajectory. Vertical dashed lines indicate times of current sheet crossing.

$$\Delta t = \frac{\Delta\lambda}{\Omega_s - \Omega_e} = \frac{\Omega_s}{\Omega_s - \Omega_e} \cdot \frac{L}{V}. \qquad (1)$$

Notice that this delay exceeds the time for the solar wind to propagate from the "source surface" to the earth's orbit: this time is equal to L/V.

Taking into consideration expression (1), each of the 3-h averages of the solar wind speed V measured by Prognoz 9 at time t was "projected" in turn onto the "source surface": $(V, t) \Rightarrow (V, t - \Delta t(V))$. The results of such a "projection" are presented in Fig. 2. These results can be interpreted as the distribution of solar wind speed along the projection of the satellite trajectory on the "source surface" (dashed line in Fig. 1), the distribution being calculated in the kinematic approximation (noninteracting particles). In Fig. 2 (as in Fig. 1), hatching denotes time intervals when Prognoz 9 was situated in the northern hemisphere of the sun relative to the heliospheric current sheet. Transition from a nonhatched to a hatched segment (and vice versa) corresponds to an intersection of the current sheet (at R_{SS}). It is easy to see from Fig. 2 that, in most cases, the solar wind speed increases with increasing distance from the current sheet.

In order to describe this effect quantitatively we will use the concept of the angular distance λ from the current sheet, defining λ as the shortest angular distance between the current sheet and the projection of the satellite position onto R_{SS} at time $t - \Delta t(V)$. We will take $\lambda < 0$ if this projection lies in the northern hemisphere relative to the current sheet, and $\lambda > 0$ if it lies in the south. We use the position of the heliospheric current sheet presented in Fig. 1 and the "projection" of the solar wind speed V onto the "source surface" in Fig. 2 to determine how V depends on the angular distance from the current layer λ. In Fig. 3 we show the results for all 1390 3-h averages of solar wind speed based on Prognoz-9 data. The stepped line in Fig. 3 shows the results of averaging V over 5°-intervals of λ.

It can be seen easily in Fig. 3 that the solar wind speed has a tendency to increase with increasing distance from the current sheet, increasing on average from 350-400 km/sec at $\lambda = 0°$ to 500-550 km/sec at $\lambda = 40°$. There does not exist any theoretical expression to describe how V should depend on λ. And since the scatter of the experimental points is very large, we can use an empirical expression to approximate $V(\lambda)$ only if we introduce a few free parameters. For example, the following empirical expressions have been used in [5, 11, 12] to describe the dependence of V on λ: $V(\lambda) = a + b\sin^2\lambda$, $V(\lambda) = a + b/\cosh(\lambda/c)$, and $V(\lambda) = a + b/\exp(\lambda/c)^2$. It can be shown that the best values of the parameters a, b, and c in these expressions (in the sense of minimizing the mean-square deviations of the experimental points in Fig. 3 from the approximate curve) are the following: V(km/sec) = $410 + 305\sin^2\lambda$, V(km/sec) = $552 - 167/\cosh(\lambda/16.3°)$, and V(km/sec) = $530 - 144/\exp(\lambda/23.4°)^2$. In the first case, the correlation coefficient $R_1 = 0.434$ is naturally somewhat smaller than in the second and third cases, where $R_2 = 0.475$ and $R_3 = 0.478$. The first and

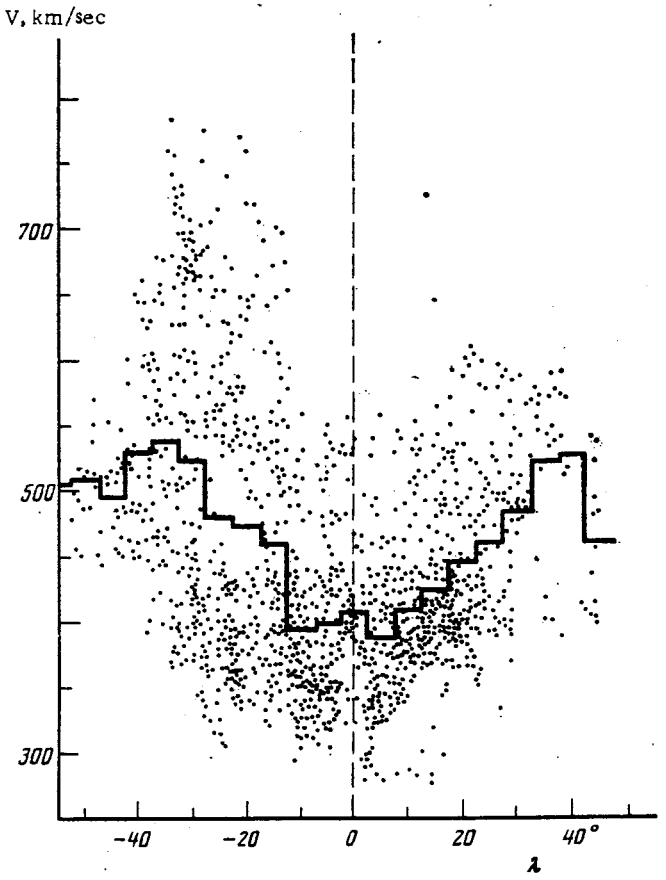

Fig. 3. Distribution of 3-h averages of solar wind speed as a function of angular distance from the current sheet.

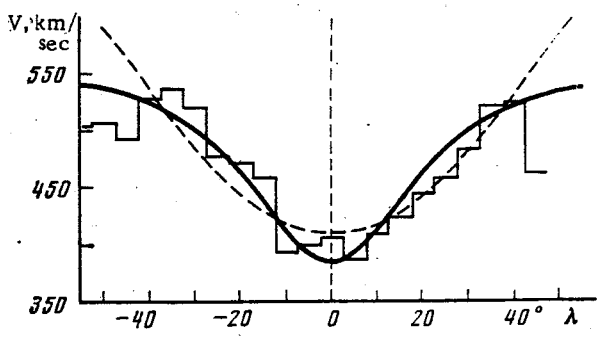

Fig. 4. Empirical dependences of solar wind speed on angular distance from the current sheet. Dashed line: $V = 410 + 305 \sin^2 \lambda$. Solid line: $V = 552 - 167/\cosh(\lambda/16.3°)$.

of the point on the "source surface" from which the solar wind was emitted. Let us suppose that the speed of the wind does not change over the distance L between the "source surface" and the earth's orbit. Then at a time when the solar wind is recorded with speed V, the difference in heliographic longitude between the earth and the source of this wind will be $\Delta\lambda = \Omega_S L/V$, where $\Omega_S = 14.18$ deg/day is the angular velocity of solar rotation. Now, the earth moves with angular velocity $\Omega_S - \Omega_e$ relative to the "source surface," where $\Omega_e = 0.98$ deg/day is the angular velocity of the earth's orbital rotation. Hence, the delay between the time when the earth passes over the source region of the solar wind (whose speed is V) and the time when the plasma emitted from that region is recorded is

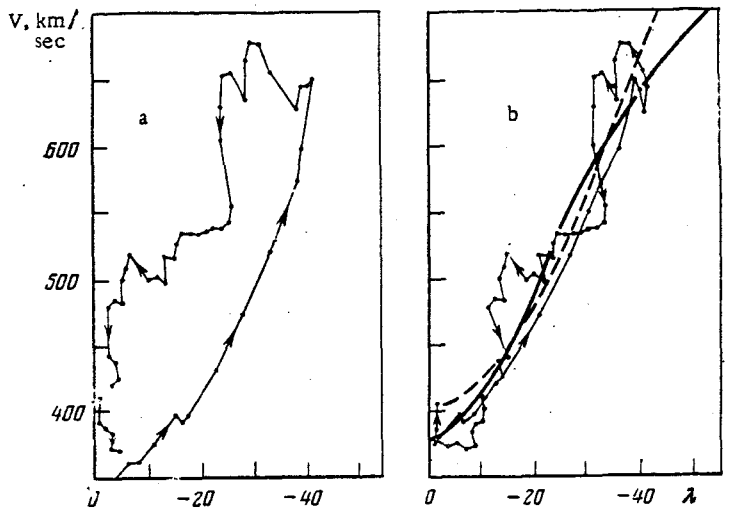

Fig. 6. Solar wind speed as a function of angular distance from the current sheet. Prognoz-9 data for the period Sept. 24-Oct. 2, 1983. In (a) we apply the condition $\langle V \rangle = V$; in (b), $\langle V \rangle = 0.85\ V$. The dashed and solid lines in (b) indicate the empirical functions $V = 401 + 664 \sin^2 \lambda$ and $V = 787 - 407/\cosh(\lambda/22.9°)$, respectively.

second empirical functions are presented in Fig. 4 as the dashed and solid lines, respectively. (The third function is not shown: its plotted version differs very little from the plotted version of the second function.) For comparison, we also show in Fig. 4 the results of averaging V over 5°-intervals of λ (as in Fig. 3).

We wish to emphasize the following feature of the solar wind distribution "projected" onto the "source surface." It can be seen in Fig. 2 that, on average, the greatest value of V is not achieved at maximum distance from the current sheet, but rather closer to the point of exit from either the northern or the southern hemisphere of the sun (relative to the interplanetary current sheet). This fact seems to be related to the following point: the mean solar wind speed $\langle V \rangle$ from R_{SS} to the satellite is less than the value of V which is measured at the earth's orbit:

$$\langle V \rangle = L \Big/ \int_{R_{SS}}^{R_{SS}+L} \frac{dr}{V(r)} < V. \qquad (2)$$

In Fig. 5 we present a comparison of the results of "projecting" the solar wind speed onto the "source surface," but instead of using V in Eq. (1), we use $\langle V \rangle = V$ in the first case and $\langle V \rangle = 0.85\ V$ in the second case. It is clear from this comparison that, in the latter case, the V profile is situated more symmetrically relative to the times of current sheet crossing.

When we use the assumption $\langle V \rangle < V$ to "project" onto the "source surface," this eliminates to some extent the hysteresis in the $V(\lambda)$ function: the hysteresis is associated with the asymmetric V profile relative to the times of current sheet crossing when $\langle V \rangle = V$. In Fig. 6 we show how the solar wind speed depends on the angular distance from the current sheet λ for the same time interval as in Fig. 5. As before, the two panels in Fig. 6 refer to the two cases $\langle V \rangle = V$ and $\langle V \rangle = 0.85\ V$. It is obvious that, in the second case, the "hysteresis" in the $V(\lambda)$ function is practically eliminated: the ascending and descending branches of the function are situated substantially closer to each other. In the case $\langle V \rangle = 0.85\ V$, the scatter of the experimental points with respect to the empirical expressions $V(\text{km/sec}) = 401 + 664 \sin^2 \lambda$ and $V(\text{km/sec}) = 787 - 407 \cosh(\lambda/22.9°)$ is relatively small (Fig. 6). For these expressions, the correlation coefficients are equal to $R_1 = 0.93$ and $R_2 = 0.94$, respectively. In practice, these coefficients indicate that the connection between the quantities is functional rather than correlative.

2. Discussion. In recent years, about ten publications have appeared dealing with the dependence of solar wind speed on angular distance from the current sheet. In the pres-

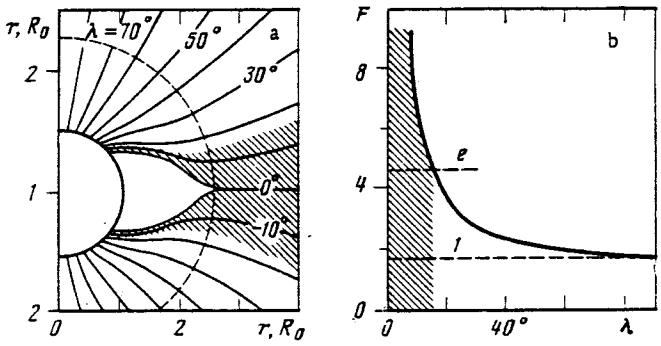

Fig. 7. a) Simplified model of the magnetic-field distribution in the vicinity of the sun: dashed line denotes the "source surface." b) Expansion factor of a tube of force F for the simplified model at great distances from the sun. We show the smallest value of the factor (1) and the factor which exceeds it by a factor of e.

ent paper, the technique is most similar to that in [4]. The authors of [4] have also used the calculations of heliospheric current sheet position performed in [13] on the basis of measurements of the photospheric magnetic field at the Stanford solar observatory, and "projected" onto the "source surface" by using the solar wind speed which is measured at the earth's orbit.

The correlation dependence V(km/sec) = 408 + 473 $\sin^2\lambda$ (R = 0.384) which was obtained in [4] is somewhat steeper than the one we have obtained here [V(km/sec) = 410 + 305 $\sin^2\lambda$ (R = 0.434)]. The dependence obtained in [4] was extracted from data gathered during the minimum of solar cycle No. 20, from May 1976 to August 1977. However, the scatter of the initial data is rather large (see Fig. 4a in [4] and Fig. 3), and so it is hardly advisable to claim that this difference is related to the different phases in the solar cycle. The same conclusion can be drawn from the analysis performed in [5].

In general, it is extraordinarily difficult to make comparisons between the expressions obtained by different authors for the function $V(\lambda)$: nonuniformities in the initial material are large. For example, some authors do not use only direct measurements of V, but also make use of solar wind speeds measured by means of interplanetary scintillations [11]. Or else the position of the interplanetary current sheet is determined from curves of maximum K-corona brightness, or is selected in such a way as to fit the observed solar wind speeds [12, 2, 11]. There are also great differences between the methods used to determine λ in different papers. Although we need to keep in mind the differences in techniques outlined above, we present here the results of other determinations of the function $V(\lambda)$: V(km/sec) = 400 + 1000 $\sin^2\lambda$ [2], V(km/sec) = 350 + 800 $\sin^2\lambda$, for $\lambda < 35°$, and equal to 600 for $\lambda > 35°$ [11], V(km/sec) = 1000 − 700/cosh(λ/16.7°) [12], and V(km/sec) = 624 − 241/exp$(\lambda/15°)^2$ [5].

It is easy to convince oneself that as long as the values of λ are not too large, the numerical values of V obtained from all of the above functional forms for $V(\lambda)$ are quite similar. However, the shallowest function is that obtained from the Prognoz-9 data set. There can be no doubt about the fact that we have established an increase in V with increasing λ. However, we cannot yet regard as clearly established the quantitative characteristics of this increase, or how it depends on conditions in the solar corona.

The principal reason which prevents us from establishing precisely the quantitative characteristics of the function $V(\lambda)$ is that it is difficult to separate spatial from temporal variations in the solar wind speed at 1 A.U. The spatial variations are associated with distance from the current sheet; the temporal variations are due to the presence of transients. Direct usage of the entire data set of V measurements leads to quite a large scatter in the experimental points relative to the approximate curve (Fig. 3). Consequently, its shape is distorted. In [14], segments of the solar wind speed data set associated with transients were eliminated, and this led to an improved correlation between V and λ, even during the period of maximum activity in 1979.

Another way to reduce the effects of transients in the solar wind and in the solar corona on the form of $V(\lambda)$ is to analyze this function just as we have done in this paper for the Prognoz-9 solar wind measurements during a comparatively short time interval (Fig. 6,

for the period Sept. 24-Oct. 2, 1983). It can be seen from Fig. 6 that when we allow for the acceleration of the solar wind at $r > R_{ss}$, there is a substantial reduction in the scatter of the points with respect to the approximate curve: the curve also becomes steeper.

In the present paper we have not solved the problem of optimizing the integrated characteristic of the solar wind acceleration process $\langle V\rangle/V$. This problem may also be solved by analyzing individual intervals of solar wind measurements. In fact, the ratio $\langle V\rangle/V$ can be considered as an additional free parameter and one can choose its magnitude so as to minimize the rms deviation of the experimental points from the approximate curve (Fig. 6).

In [10, 14], the authors do not study only the function $V(\lambda)$: they also investigate how the solar wind speed depends on the radial component of the magnetic field B_r at the "source surface" R_{ss}. In principle, there is no difference between these two approaches, because the distribution of λ and the distribution of B_r along the projection of the satellite trajectory at R_{ss} are both calculated in the potential approximation on the basis of identical measurements of the photospheric magnetic fields. Both of these quantities are minimal in the vicinity of the current sheet, and both increase as one moves away from the sheet.

In conclusion, we will dwell briefly on the physical processes which determine the shape of the minimum in solar wind speed in the vicinity of the interplanetary current sheet. It can be seen from the data presented in Figs. 3, 4, and 6 that the characteristic angular width of the $V(\lambda)$ profile in the vicinity of the heliospheric current sheet is ~30-40°. At 1 A.U. this corresponds to $\sim 10^8$ km. A formation on a scale as large as this is apparently determined by the global hydrodynamic expansion of the solar corona as a whole.

To illustrate this point, we show in Fig. 7a a simplified model of the magnetic-field distribution in the vicinity of the sun (this is also the distribution of current lines in the plasma):

$$B_r = \frac{2M\sin\lambda}{R_s^3}\left[\left(\frac{R_s}{r}\right)^3 + \frac{1}{2}\left(\frac{R_s}{R_{ss}}\right)^3\right], \quad B_\lambda = \frac{M\cos\lambda}{R_s^3}\left[\left(\frac{R_s}{r}\right)^3 - \left(\frac{R_s}{R_{ss}}\right)^3\right]. \tag{3}$$

This field satisfies the Laplace equation for $R_s < r < R_{ss}$, it satisfies the condition of constant magnetic potential on $r = R_{ss}$, and it is similar to the dipole field at $r = R_s$. In Fig. 7b we show the areal expansion factor of a tube of force of the magnetic field $F = S(R_{ss})R_s^2/R_{ss}^2S(R_s)$ as a function of the angular distance λ from the current sheet. It can be seen from this figure that within the framework of the model in Eq. (3) the expansion factor is practically constant for $|\lambda| > 30°$, but it increases very rapidly in the neighborhood of the current sheet, $|\lambda| \leq 15°$. The characteristic angular size of the region where the expansion factor is large (~±15°, shown as a hatched region in Fig. 7) is similar to the characteristic angular width of the $V(\lambda)$ profile in the neighborhood of the heliospheric current sheet, ~30°.

Generally speaking, processes are observed on three different scales in the vicinity of the interplanetary current sheet at 1 A.U. For many sector boundaries, the change in the direction of the magnetic field occurs over an interval of ~1 min. For other sector boundaries it may take the spacecraft ~1 h or more to intersect the boundary. The corresponding distance scales are 10^4-10^6 km. The solar wind density is observed to increase in the vicinity of the heliospheric current sheet (noncompressive density enhancement NCDE): the characteristic duration of such increases is ≈0.5 day [15], corresponding to a spatial scale of $(1\text{-}2)\cdot 10^7$ km. We have already mentioned that the spatial scale of the minimum in V is $\sim 10^8$ km. If the spatial scale of the minimum in V determines the global hydrodynamics of the solar corona, and the spatial scale of the jump in magnetic field at the current sheet is determined by plasma processes occurring in the vicinity of the sheet, then it is not clear what processes are responsible for the formation of NCDE in the vicinity of the interplanetary current sheet with intermediate characteristic scale sizes.

CONCLUSIONS

We have investigated quantitatively how the solar wind speed V depends on the angular distance λ from the interplanetary current sheet. As a basis for the investigation, we have used measurements of the solar wind made by Prognoz 9 between July 1983 and February 1984 on the declining phase of solar cycle No. 21.

Using the entire data set of V measurements from Prognoz 9, the function $V(\lambda)$ can be approximated by the following empirical expression: $V(km/sec) = 410 + 305 \sin^2 \lambda$ (see also Sec. 1).

We have shown that the scatter in the experimental points relative to the approximate curve can be reduced by assuming that along the path length L from the "source surface" R_{ss} to the earth's orbit, the mean solar wind speed $\langle V \rangle = L \Big/ \int_{R_{ss}}^{R_{ss}+L} \frac{dr}{V(r)}$ is less than the value of V measured at 1 A.U.

We have proposed a method of estimating the ratio <V>/V (i.e., an integral characteristic of the solar wind acceleration process) based on measurements of solar wind parameters at 1 A.U.

LITERATURE CITED

1. K. I. Gringauz, V. V. Bezrukikh, M. I. Verigin, and G. A. Kotova, "Recurrent high-speed streams in the solar wind during the decay phase of solar cycle No. 21: observations with a wide-angle ion energy spectrometer on Prognoz 9," Kosm. Issled. (this issue).
2. X.-P. Zhao and A. J. Hundhausen, "Organization of solar wind plasma properties in a tilted heliomagnetic coordinate system," J. Geophys. Res., 86, No. A7, 5423 (1981).
3. B. J. Rickett and W. A. Coles, "Solar cycle evolution of the solar wind in three dimensions," in: Solar Wind Five, M. Neugebauer (ed.), NASA CP-2280, Washington, DC (1983), p. 315.
4. K. Hakamada and Y. Munakata, "A cause of the solar wind speed variations: an update," J. Geophys. Res., 89, No. A1, 357 (1984).
5. G. Newkirk, Jr. and L. A. Fisk, "Variation of cosmic rays and solar wind properties with respect to the heliospheric current sheet. 1. 5-GeV protons and solar wind speed," J. Geophys. Res., 90, No. A4, 3391 (1985).
6. N. Crooker, "Solar cycle variations of the solar wind," in: Solar Wind Five, M. Neugebauer (ed.), NASA CP-2280, Washington, DC (1983), p. 303.
7. Yu. D. Krisilov, V. V. Bezrukikh, et al., "A wide-angle charged-particle energy spectrometer for investigating the solar wind on Prognoz 9," in: Scientific Instruments for Space Research [in Russian], Nauka, Moscow (1986).
8. K. H. Schatten, J. M. Wilcox, and N. F. Ness, "A model of interplanetary and coronal magnetic fields," Solar Phys., 6, No. 3, 442 (1969).
9. M. D. Altschuler and G. Newkirk, Jr., "Magnetic fields and the structure of the solar corona," Solar Phys., 9, No. 1, 131 (1969).
10. J. T. Hoeksema, "Structure and evolution of large-scale solar and heliospheric magnetic fields," Doctoral Dissertation, CSSA-Astro-84-07, Stanford, California (1984).
11. X.-P. Zhao and A. J. Hundhausen, "Spatial structure of solar wind in 1976," J. Geophys. Res., 88, No. A1, 451 (1983).
12. K. Hakamada and S.-I. Akasofu, "A cause of solar wind speed variations observed at 1 A.U.," J. Geophys. Res., 86, No. A3, 1290 (1981).
13. J. T. Hoeksema, J. M. Wilcox, and P. H. Scherrer, "Structure of heliospheric current sheet in the early portion of sunspot cycle 21," J. Geophys. Res., 87, No. A12, 10331 (1982).
14. S. T. Suess, J. M. Wilcox, et al., "Relationship between a potential field source surface model of the coronal magnetic field and properties of the solar wind at 1 A.U.," J. Geophys. Res., 89, No. A6, 3957 (1984).
15. G. Borrini, J. M. Wilcox, et al., "Solar wind helium and hydrogen structure near the heliospheric current sheet: a signal of coronal streamers at 1 A.U.," J. Geophys. Res., 86, No. A6, 4565 (1981).